Demonstration of electron filtering to increase the Seebeck coefficient in $In_{0.53}Ga_{0.47}As/In_{0.53}Ga_{0.28}Al_{0.19}As$ superlattices

J. M. O. Zide,[1] D. Vashaee,[2] Z. X. Bian,[2] G. Zeng,[3] J. E. Bowers,[3] A. Shakouri,[2] and A. C. Gossard[1]
[1]*Materials Department, University of California, Santa Barbara, California 93106-5050, USA*
[2]*Jack Baskin School of Engineering, University of California, Santa Cruz, California 95064, USA*
[3]*Department of Electrical and Computer Engineering, University of California, Santa Barbara, California 93106, USA*
(Received 17 April 2006; revised manuscript received 10 July 2006; published 30 November 2006)

In this paper, we explore electron filtering as a technique to increase the Seebeck coefficient and the thermoelectric power factor of heterostructured materials over that of the bulk. We present a theoretical model in which the Seebeck coefficient and the power factor can be increased in an $In_{0.53}Ga_{0.47}As$-based composite material. Experimental measurements of the cross-plane Seebeck coefficient are presented and confirm the importance of the electron filtering technique to decouple the electrical conductivity and Seebeck coefficient to increase the thermoelectric power factor.

DOI: 10.1103/PhysRevB.74.205335 PACS number(s): 73.50.Lw, 73.21.−b

Traditionally, research on thermoelectric materials has focused on finding or synthesizing materials that have a good balance of the relevant properties rather than systematic studies on how to decouple these parameters using new physical approaches. The efficiency of thermoelectric materials is quantified by the dimensionless figure of merit $ZT = S^2\sigma T/\beta$, where S is the Seebeck coefficient, σ is electrical conductivity, β is thermal conductivity, and T is temperature. Good thermoelectric materials have high electrical conductivity and Seebeck coefficients and low thermal conductivities, but these properties are not independent. In particular, the electrical conductivity and Seebeck coefficient are inversely related, so it is not generally possible to increase the thermoelectric power factor above a particular optimal value for a bulk material. Traditional thermoelectric materials, such as bismuth telluride (Bi_2Te_3) and lead telluride (PbTe), have ZT values of ~1. Pioneering work by Hicks and Dresselhaus[1,2] suggested an improvement in thermoelectric power factor for low-dimensional solids. Recent work by Venkatasubramanian *et al.*[3] and Harman *et al.*[4] using superlattices and quantum dots based on these materials has increased room temperature ZT to ~2–2.4. These improvements in performance are primarily a result of a reduction in lattice thermal conductivity, and the thermoelectric power factor ($S^2\sigma$) is largely unchanged. Shakouri *et al.* first proposed the use of solid-state thermionics for thermoelectric applications,[5] which allows the use of materials with high electrical conductivity and low thermal conductivity while relaxing the need for a high Seebeck coefficient. Mahan *et al.* first proposed multilayer thermionic emission to increase the efficiency (ZT),[6] but later concluded that the main advantage of heterostructures was in the reduction of phonon thermal conductivity.[7] Shakouri *et al.* later suggested that tall barriers and highly degenerately doped superlattices could achieve substantial increases in thermoelectric power factor over bulk materials.[8] Vashaee *et al.* revisited electron transport perpendicular to the barrier and determined that highly degenerately doped semiconductor or metal superlattices could achieve power factors higher than the bulk and determined that nonconservation of transverse momentum can have a large effect (especially in the case of metal superlattices) by increasing the number of electrons contributing to conduction by thermionic emission.[9] In this paper, we calculate the electrical and thermoelectric properties of superlattices consisting of degenerately doped $In_{0.53}Ga_{0.47}As$ with $In_{0.53}Ga_{0.28}Al_{0.19}As$ barriers. Experimental measurements show a corresponding increase in room-temperature cross-plane Seebeck coefficient. We believe this is direct experimental evidence of the importance of this electron filtering technique to increase the thermoelectric power factors of heterostructures over those of constituent bulk materials.

If barriers are incorporated into a bulk material to create a superlattice, the electron transport properties can be changed drastically. If these barriers are sufficiently thick, the electron motion through the semiconductor will be limited to those electrons with sufficiently high energy for thermionic emission over the barrier. That is, electrons will be filtered so that only high-energy electrons contribute to conduction. Using this electron filtering technique, it is possible to dramatically increase the Seebeck coefficient with a relatively modest decrease in electrical conductivity.

Mathematically, we can write the transport coefficients based on the Boltzmann transport equation as:

$$\sigma = \int \sigma(E)dE \tag{1}$$

and

$$S = \frac{1}{qT}\frac{\int \sigma(E)(E - E_F)dE}{\int \sigma(E)dE}, \tag{2}$$

where

$$\sigma(E) = q^2\tau(E)v^2(E)D(E)\left(\frac{-df}{dE}\right), \tag{3}$$

$\tau(E)$ is the energy-dependent relaxation time, which can be modified to take into account the quantum-mechanical transmission probability $T(E)$, $v(E)$ is electron velocity, $D(E)$ is the density of states, and $f(E)$ is the Fermi-Dirac distribution

TABLE I. Parameters used in the simulations of $In_{0.53}Ga_{0.47}As/In_{0.53}Ga_{0.28}Al_{0.19}As$ superlattice, where n_w is the number of wells. L_w and L_b are well and barrier widths, respectively. E_b is the barrier height. β, μ_b, α, and V_s are thermal conductivity, electron mobility in the barrier region, nonparabolicity coefficient, and the saturation velocity, respectively. Mobility in the well region depends on the doping concentration and has been fit to experimental measurements.

Well/barrier	n_w	L_w (nm)	L_b (nm)	E_b (meV)	m_{eff} (well/barrier)	β (300 K) (W/mK) (bulk/SL)	β (900 K) (W/mK) (bulk/SL)	μ_b (cm^2/V s)	V_s (cm/s)	α (eV^{-1})
$In_{0.53}Ga_{0.47}As/In_{0.53}Ga_{0.28}Al_{0.19}As$	70	20	10	200	0.043/0.058	5.5 / 3.5	2.5 / 2.1	5600	2×10^7	1.167

function. If the barriers of a heterostructure are sufficiently thick to neglect the contribution of tunneling, it is possible to use a Heaviside step function approximation: $T(E)\approx\Theta(E-E_B)$, where E_B is the barrier energy. If transverse momentum (i.e., momentum in the xy plane where the z direction is the periodic direction of the superlattice) is conserved (i.e., no elastic scattering of momentum in the xy plane into the z direction), then $T\approx\Theta([h^2k_z^2/2m]-E_B)$ and only electrons with sufficient momentum perpendicular to the barriers contribute to the conduction. If transverse momentum is not conserved, motion in the xy plane is coupled to motion in the z direction and $k^2=k_x^2+k_y^2+k_z^2$. In this case, $T\approx\Theta([h^2k^2/2m]-E_B)$, and a larger differential conductivity results. Vashaee *et al.* have shown theoretically that nonconservation of transverse momentum can greatly increase thermionic emission current and, comparing their model to experimental current-voltage characteristics of various superlattice structures, found that transverse momentum is conserved for electrons in planar semiconductor barriers.[9,10] The conservation of transverse momentum is a consequence of the relative translational invariance in the plane of a conventional quantum well. By controlling the roughness of the superlattice interfaces during the growth or by taking advantage of well-designed quantum dot structures, it is possible to break this translational invariance and increase the thermionic current density and consequently the electrical conductivity.

In this work, we present a model for $In_{0.53}Ga_{0.47}As$ wells with $In_{0.53}Ga_{0.28}Al_{0.19}As$ barriers with a Ga/Al ratio chosen for a barrier height of E_B=200 meV. Parameters used for these calculations are given in Table I. Briefly, a conventional bulk transport was modified to calculate the in-plane and cross-plane thermoelectric characteristics of the superlattice structures.[10] The quantum-mechanical transmission coefficient for electron transport between wells was introduced in the Boltzmann equation to take into account both tunneling and thermionic emission. The contributions in transport from 2D states in the well and 3D states above the well and in the barrier region are considered separately. Since the barrier layer thickness is large enough for miniband transport to be negligible, the transmission probability is calculated using the Wentzel-Kramers-Brillouin (WKB) approximation. Finally, Fermi-Dirac statistics were used to account for the number of available empty states in the neighboring wells for tunneling and thermionic emission calculations.

Calculations are performed assuming both conservation and nonconservation of transverse momentum. Room-temperature results are given in Fig. 1. Of the increase in the peak value of ZT, approximately 65% is due to electron filtering, while the remaining 35% is due to reduced thermal conductivity because of phonon scattering by the ErAs nanoparticles in the $In_{0.53}Ga_{0.47}As$ which has been experimentally measured and discussed elsewhere.[11,12] It is worth noting that

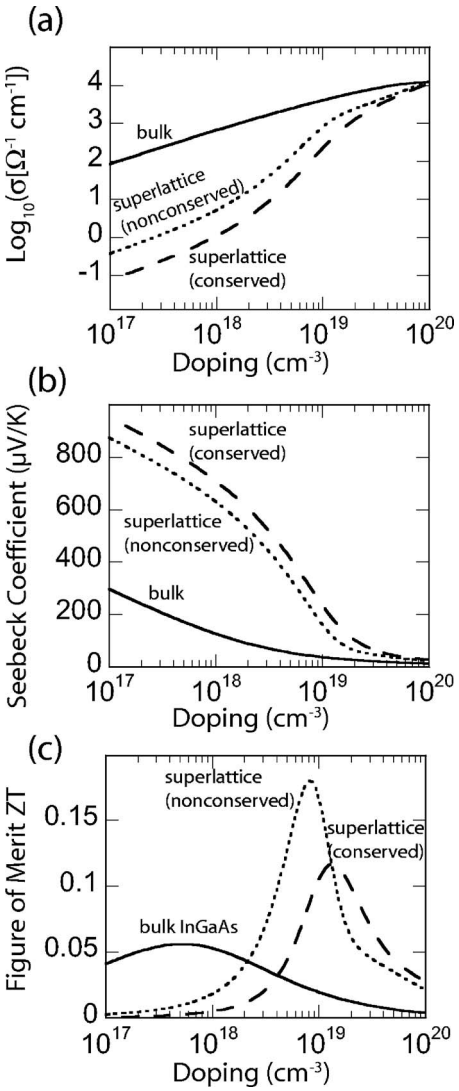

FIG. 1. Room-temperature modeling of cross-plane electrical and thermoelectric properties: (a) electrical conductivity, (b) Seebeck coefficient, and (c) ZT. Solid curves are bulk $In_{0.53}Ga_{0.47}As$, while dashed curves are superlattices with conserved transverse momentum and dotted curves are superlattices with nonconserved transverse momentum.

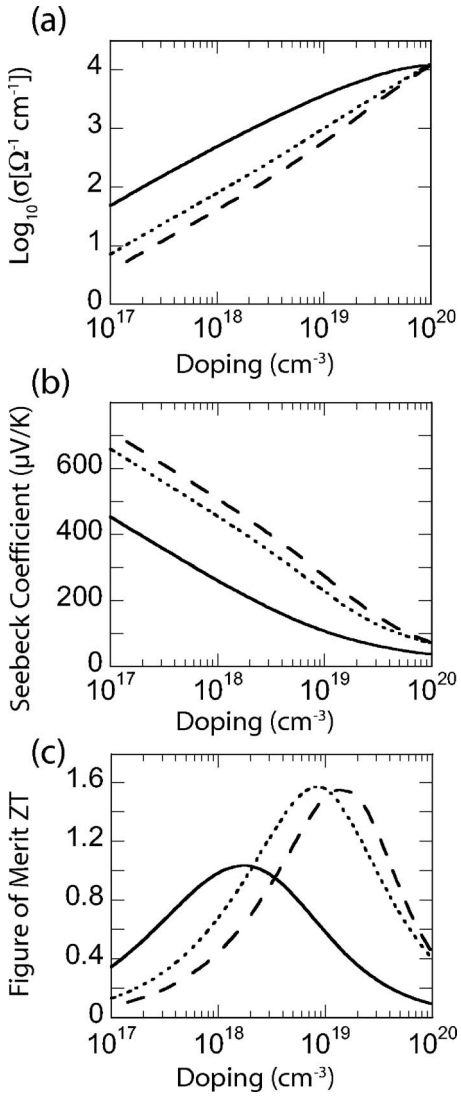

FIG. 2. High-temperature (900 K) modeling of cross-plane electrical and thermoelectric properties: (a) electrical conductivity, (b) Seebeck coefficient, and (c) *ZT*. Solid curves are bulk $In_{0.53}Ga_{0.47}As$, while dashed curves are superlattices with conserved transverse momentum and dotted curves are superlattices with nonconserved transverse momentum.

the peak values occur at different doping densities; electron filtering allows higher doping densities to be used while still increasing the Seebeck coefficient. In this way, the thermoelectric power factor is increased. In Fig. 2, similar results are presented at higher temperatures (900 K), where the thermoelectric figure of merit for these materials is expected to be higher. In this case, approximately 84% of the increase in peak *ZT* is due to electron filtering, while the remainder is due to decreased thermal conductivity. These materials are stable at high temperatures with proper surface passivation.

To test this model experimentally, several $In_{0.53}Ga_{0.47}As/In_{0.53}Ga_{0.28}Al_{0.19}As$ samples (lattice-matched to InP) were grown on both (100) semi-insulating InP:Fe and (100) *n*-type InP:Sn substrates using a Varian Gen II molecular-beam epitaxy (MBE) system. In each case, the substrate temperature was measured at 490 °C using a pyrometer. A schematic representation of the sample structure is given in Fig. 3. In each sample, the 20 nm $In_{0.53}Ga_{0.47}As$ regions contain 0.3 at. % of codeposited ErAs nanoparticles. ErAs is a semimetal that forms self-assembled nanoparticles in a rocksalt structure when incorporated into MBE-grown $In_{0.53}Ga_{0.47}As$.[13] The incorporation of ErAs into semiconductors can have effects including the creation of a buried Schottky barrier,[14] the creation of deep states for rapid carrier recombination,[15] enhanced tunneling,[16] doping,[17] or phonon scattering[18,19] to reduce thermal conductivity.[11,12] In this work, ErAs is included as an electron donor and a phonon scattering center for reduced thermal conductivity. Codoping with ErAs in addition to silicon makes it possible to achieve a large bulk doping (10^{19} cm^{-3}) without special efforts and generally results in a larger mobility than $In_{0.53}Ga_{0.47}As$, which is equivalently doped with silicon. Also, it is hoped that the incorporation of ErAs into the $In_{0.53}Ga_{0.47}As$ will result in nonconservation of transverse momentum, and consequentially higher electrical conductivity and *ZT*. The effects of ErAs on the thermoelectric properties of $In_{0.53}Ga_{0.47}As$ and details of the growth of the $In_{0.53}Ga_{0.47}As$ region are given elsewhere.[20]

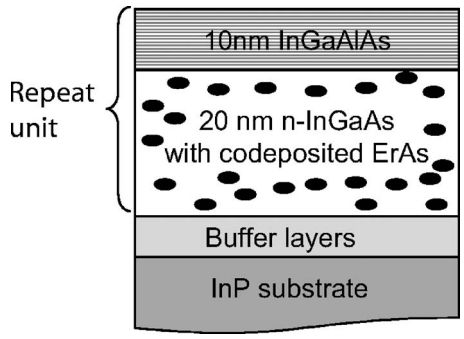

FIG. 3. Schematic diagram of the sample structure. Each sample structure was grown on both semi-insulating substrates for in-plane measurements (30 repeat units) and on conductive (*n*-type) substrates (70 repeat units) for cross-plane measurements. Samples were doped with both ErAs and varying amounts of silicon.

The barrier layers consist of 10 nm of $In_{0.53}Ga_{0.28}Al_{0.19}As$, which is grown as a short-period superlattice (~1 nm period), consisting of $(In_{0.53}Ga_{0.47}As)_{0.6}(In_{0.52}Al_{0.48}As)_{0.4}$. This type of short-period superlattice is quantum mechanically equivalent to a conventional alloy of the same composition and total thickness. This technique is commonly used to simplify the growth of structures containing both $In_{0.53}Ga_{0.47}As$ and $In_{0.53}Ga_{0.28}Al_{0.19}As$. In this case, the barrier layers can be effectively considered to be identical to conventional $In_{0.53}Ga_{0.28}Al_{0.19}As$ barriers with a height of ~200 meV.

The $In_{0.53}Ga_{0.47}As$ regions are codoped with varying amounts of silicon, resulting in samples with $In_{0.53}Ga_{0.47}As$ electron concentrations of 2, 4, 6, and 10×10^{18} cm^{-3}. The electron concentration of these samples was measured using the samples grown on semi-insulating substrates using room-temperature Hall measurements in a van der Pauw geometry. The free-electron concentrations, obtained by dividing the measured sheet carrier densities by the total thickness of $In_{0.53}Ga_{0.47}As$ in the structure, and the corresponding electron mobilities are plotted in Fig. 4.

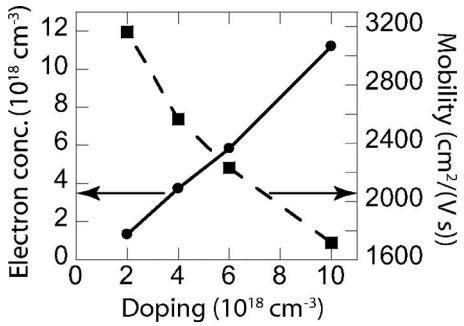

FIG. 4. Room-temperature, in-plane electrical properties of the ErAs:$In_{0.53}Ga_{0.47}As$ wells as a function of ErAs doping plus silicon codoping. Electron concentration, solid line and filled circles; and electron mobility, dashed line and filled squares.

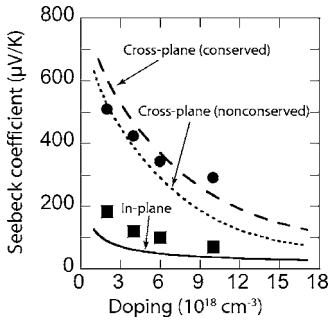

FIG. 5. Room-temperature Seebeck coefficient; comparison of experimental and theoretical data in the in-plane (experimental data: squares, theory: solid curve) and cross-plane directions (experimental data: circles, theory: dashed curve for a superlattice with conserved transverse momentum and dotted curve for a superlattice with nonconserved transverse momentum). Experimental results indicate an improvement in the Seebeck coefficient due to electron filtering.

Using the samples grown on semi-insulating substrates, the room-temperature in-plane Seebeck coefficient was measured for each effective doping concentration. A thermoelectric cooler was used to create a temperature gradient across a small sample of each structure. Metal contacts were deposited and the differences in voltage and temperature (the ratio being the Seebeck coefficient) were measured. The in-plane Seebeck coefficients are plotted in Fig. 5 and compared to theoretical values for bulk ErAs:$In_{0.53}Ga_{0.47}As$ obtained using the model we have described.

The cross-plane Seebeck coefficient, which should be larger than the in-plane Seebeck coefficient because of the electron filtering effect, was measured using the samples grown on *n*-type substrates, in which the superlattice thickness was 2.1 μm. Mesas were etched to isolate the superlattice, and metal contacts were deposited on the mesa. A dielectric layer was deposited on top of the structure and a microheater was fabricated. The same structures were fabricated on the substrate (with the superlattice etched away) and the combined Seebeck coefficient of the superlattice and substrate was measured by measuring the voltage and temperature difference between the two structures. The Seebeck coefficient of the substrate was measured by a similar technique, and the Seebeck coefficient of the superlattice was extracted.[21] The resulting cross-plane Seebeck coefficients are plotted in Fig. 5 and compared to the theoretical values for electron filtering both with conserved and with nonconserved transverse momentum. The measured Seebeck values agree reasonably well with theoretical values, although it is impossible to draw conclusions as to whether transverse momentum is conserved on the basis of these measurements. Because conservation of transverse momentum is of great importance to the electrical conductivity in the cross-plane direction, further experimentation is required to determine whether the introduction of ErAs nanoparticles results in nonconservation of transverse momentum.

Thus, we have shown that electron filtering results in an increase in Seebeck coefficient by a factor of 2 to 3, and we demonstrated the importance of this technique to increase both the thermoelectric power factor and *ZT* of heterostructured materials over that of the bulk. This is accomplished by changing the differential conductivity of the material (as a function of electron energy) to decouple the electrical conductivity and the Seebeck coefficient. This approach is compatible with the reduction of thermal conductivity due to phonon scattering by ErAs nanoparticles. While further experimental evidence is required to experimentally determine the effect of electron filtering on the power factor of these materials, we have shown that this technique offers both a viable approach to more efficient thermoelectric materials and opportunities to obtain new insights into electron and heat transport in semiconductor heterostructures.

This work was supported by the Office of Naval Research as part of the Thermionic Energy Conversion MURI.

[1] L. D. Hicks and M. S. Dresselhaus, Phys. Rev. B **47**, 12727 (1993).
[2] L. D. Hicks, T. C. Harman, and M. S. Dresselhaus, Appl. Phys. Lett. **63**, 3230 (1993).
[3] R. Venkatasubramanian, E. Siivola, T. Colpitts, and B. O'Quinn, Nature (London) **413**, 597 (2001).
[4] T. C. Harman, P. J. Taylor, M. P. Walsh, and B. E. LaForge, Science **297**, 2229 (2002).
[5] A. Shakouri and J. E. Bowers, Appl. Phys. Lett. **71**, 1234 (1997).
[6] G. D. Mahan and L. M. Woods, Phys. Rev. Lett. **80**, 4016 (1998).
[7] C. B. Vining and G. D. Mahan, J. Appl. Phys. **86**, 6852 (1999).
[8] A. Shakouri, C. LaBounty, P. Abraham, J. Piprek, and J. E. Bow-

ers, in *Thermoelectric Materials—The Next Generation Materials for Small-Scale Refrigeration and Power Generation Applications*, edited by T. M. Tritt, H. B. Lyon, Jr., G. Mahan, and M. G. Kanatzidis, Materials Research Society Proceedings No. 545 (MRS, Pittsburgh, 1999), p. 449.

[9] D. Vashaee and A. Shakouri, Phys. Rev. Lett. **92**, 106103 (2004).

[10] D. Vashaee and A. Shakouri, J. Appl. Phys. **95**, 1233 (2004).

[11] W. Kim, J. Zide, A. Gossard, D. Klenov, S. Stemmer, A. Shakouri, and A. Majumdar, Phys. Rev. Lett. **96**, 045901 (2006).

[12] W. Kim, S. L. Singer, A. Majumdar, D. Vashaee, Z. X. Bian, A. Shakouri, G. Zeng, J. E. Bowers, J. M. O. Zide, and A. C. Gossard, Appl. Phys. Lett. **88**, 242107 (2006).

[13] D. O. Klenov, D. C. Driscoll, A. C. Gossard, and S. Stemmer, Appl. Phys. Lett. **86**, 111912 (2005).

[14] A. Dorn, M. Peter, S. Kicin, T. Ihn, K. Ensslin, D. Driscoll, and A. C. Gossard, Appl. Phys. Lett. **82**, 2631 (2003).

[15] C. Kadow, S. B. Fleischer, J. P. Ibbetson, J. E. Bowers, and A. C. Gossard, Appl. Phys. Lett. **75**, 3548 (1999).

[16] P. Pohl, F. H. Renner, M. Eckardt, A. Schwanhausser, A. Friedrich, O. Yuksekdag, S. Malzer, G. H. Dohler, P. Kiesel, D. Driscoll, M. Hanson, and A. C. Gossard, Appl. Phys. Lett. **83**, 4035 (2003).

[17] D. C. Driscoll, M. Hanson, C. Kadow, and A. C. Gossard, Appl. Phys. Lett. **78**, 1703 (2001).

[18] D. G. Cahill, W. K. Ford, K. E. Goodson, G. D. Mahan, A. Majumdar, H. J. Maris, R. Merlin, and S. R. Phillpot, J. Appl. Phys. **93**, 793 (2003).

[19] D. G. Cahill, K. Goodson, and A. Majumdar, J. Heat Transfer **124**, 223 (2002).

[20] J. M. Zide, D. O. Klenov, S. Stemmer, A. C. Gossard, G. Zeng, J. E. Bowers, D. Vashaee, and A. Shakouri, Appl. Phys. Lett. **87**, 112102 (2005).

[21] G. H. Zeng, J. E. Bowers, J. M. O. Zide, A. C. Gossard, W. Kim, S. Singer, A. Majumdar, R. Singh, Z. Bian, Y. Zhang, and A. Shakouri, Appl. Phys. Lett. **88**, 113502 (2006).